Constant Temperature Induced Stresses in Evacuated Enclosures for High Performance Flat Plate Solar Thermal Collectors

Paul. Henshall [a,*], Philip. Eames [a], Farid Arya [b], Trevor Hyde [b], Roger Moss [c], Stan Shire [c]

[a] Centre for Renewable Energy Systems Technology, Loughborough University, UK

[b] School of the Built Environment, University of Ulster, UK

[c] School of Engineering, University of Warwick, UK

ABSTRACT

A flat-plate solar thermal collector's efficiency can be much improved if the enclosure in which the solar absorber is housed can be evacuated. This would result in a high performance, architecturally versatile solar thermal collector capable of supplying clean energy efficiently for use in applications including residential water and space heating. This paper focuses on the design of evacuated enclosures for flat-plate solar collectors, in which the solar absorber is completely surrounded by a thin layer (4-10mm) of thermally insulating vacuum, resulting in a thin solar thermal collector (depth < 20mm). The expectations, requirements and applications of these solar collectors are discussed along with a description of the enclosure concept under consideration. Potential seal materials are identified and their limitations discussed. Finite element modelling results are presented of a study investigating how such enclosures are mechanically stressed when subject to atmospheric pressure loading and differential thermal expansion of dissimilar components. Finite element model predictions are validated against preliminary experimental strain measurements for existing experimental enclosures. It is demonstrated that with a suitably low temperature sealing process vacuum enclosure concepts can successfully withstand imposed stresses.

Keywords: renewable energy, solar thermal, vacuum, stress

1 INTRODUCTION

Solar thermal collectors conventionally come in two main forms; non-evacuated, glazed, flat-plate (FP) collectors and evacuated tube (ET) collectors. FP collectors have a larger solar absorber area to gross area ratio when compared with ET collectors but their thermal performance is poorer, especially at elevated temperatures. This is due to FP collectors typically employing a solar absorbing plate (see Figure 1) that fills a large proportion of the collector area while ET collectors employ absorbing tubes which are individually enclosed in larger evacuated glass tubes. FP collectors, however, lose heat both by convection of the internal air (or gas) and conduction through it; these modes of heat loss do not occur in a vacuum and subsequently the thermal performance of ET collectors is enhanced. Research in solar thermal collectors is therefore seeking to combine the benefits of ET and FP collectors (Benz and Beikircher, 1999).

* Corresponding author. Tel.: +44 1509 635336. Email address: p.henshall@lboro.ac.uk
FP – Flat Plate, ET – Evacuated Tube, VFP – Vacuum Flat Plate

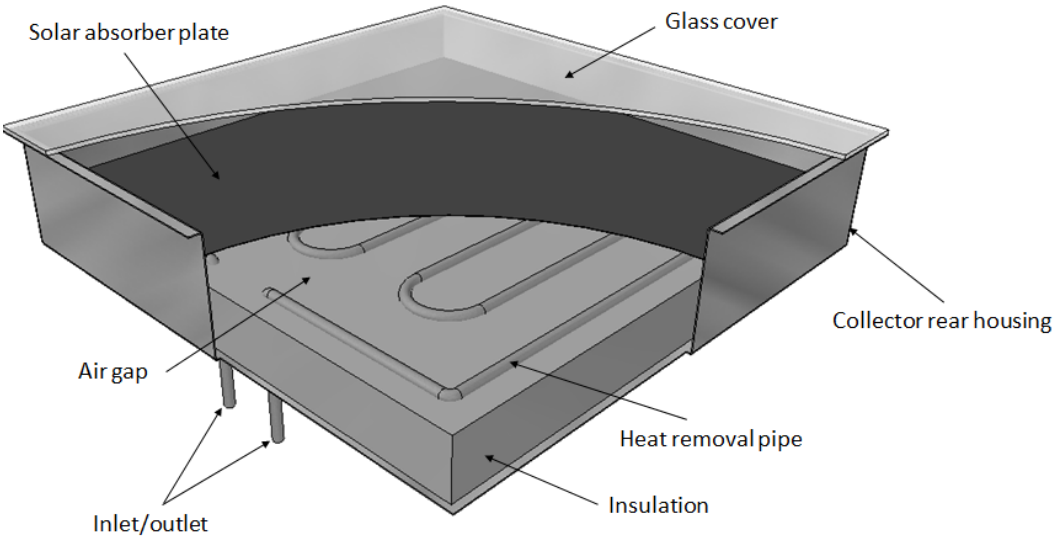

Figure 1: Depiction of a conventional flat plate solar thermal collector

There are various examples of successfully demonstrated low pressure flat-plate solar collectors in the literature, such as the work by Benz and Beikircher (1999), who successfully demonstrated a prototype flat-plate solar collector for process steam production with the collector interior filled with a low pressure krypton gas to reduce convective heat loss. A number of low pressure/vacuum flat-plate solar collectors are starting to become commercially available (TVP-Solar, n.d.). It is anticipated that a vacuum flat-plate (VFP) solar collector will exhibit greater efficiencies at higher temperatures in comparison to standard FP collectors and provide better use of available installation area in comparison to ET collectors by capturing a greater fraction of available solar radiation Furthermore if the depth of flat plate systems can be reduced to 20-50mm, increased building fabric integration is also facilitated. A concept drawing of a VFP collector is presented in Figure 2.

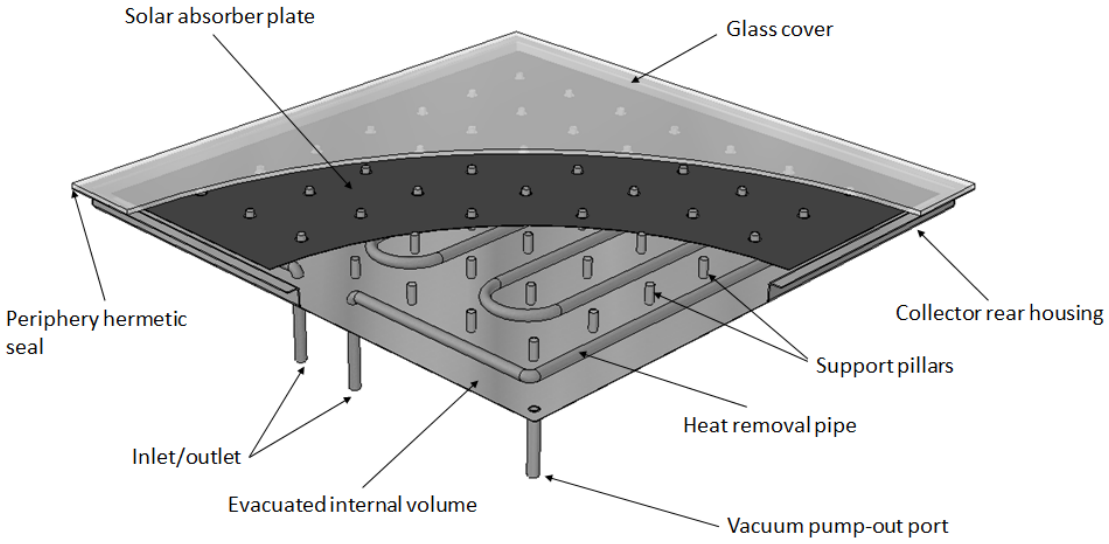

Figure 2: Conceptual depiction of a vacuum flat-plate solar thermal collector

The mechanical design of a VFP collector must be able to withstand atmospheric pressure forces applied to its exterior surface. Mechanical stress in flat, rectangular, evacuated enclosures has been investigated previously for vacuum glazing applications (Fischer-Cripps et al., 1995; Simko et al., 1998; Wang et al., 2007). Vacuum glazing consists of two sheets of glass placed together with an array of small structural support pillars separating them. The support pillars are very small, typically less than 0.5mm in both height and diameter. A seal is made around the periphery of the two glass sheets and the small interior volume is evacuated to a high vacuum (less than 0.1 Pa); this results in a narrow building component with a U-value as low as <1 W/m^2K if low emissivity coatings are used to suppress radiative heat transfer. However, the two glass sheets are subject to large stresses resulting from atmospheric pressure loading over the glass surface and differential thermal expansion when one glass sheet is warmer or cooler than the other.

Evacuated enclosures for flat-plate solar thermal collectors will have similarities in their design to the configuration of vacuum glazing described. Evacuated enclosures for flat-plate solar thermal collectors are subject to different design constraints and operational conditions with a greater variety of mechanical design options being possible. It is the purpose of this paper to explore a selection of fundamental design options and describe how such choices impact the mechanical stresses which the enclosure is subject to. One option is to employ a thin, flexible metal backing to the collector housing as opposed to using a glass cover on either side of the enclosure. This could more easily allow the use of tempered glass to form the front surface of the collector enclosure housing. Tempered glass has the advantage of being stronger and safer than standard annealed glass but due to its fabrication process is subject to the roller wave effect (PressGlass, n.d.), which causes its surface to undulate. The process of sealing a vacuum glazing and ensuring the support pillar array is evenly distributing mechanical stresses over the glass surface, although theoretically possible, is significantly more complex when using tempered glass and it is likely that this complexity extends to vacuum enclosures for flat plate solar collectors that have a front and rear glass cover. Although, such enclosures, which would be in places transparent and transmit a fraction of the incident light, could be appealing architecturally. An enclosure for a flat-plate solar collector is not subject to the requirement to have glass on both sides of the enclosure. If one side of the enclosure was fabricated from thin flexible metal, the natural flexibility of the metal could automatically compensate for the undulating surface of the tempered glass.

Using a 3D finite element method (FEM) analysis software package (ABAQUS) a parametric study was conducted to provide understanding of the mechanical stresses experienced by this evacuated enclosure concept. Mechanical stresses are characterised for both i) different enclosure sizes and ii) when the enclosure is exposed to extreme winter temperatures. FEM models are validated against preliminary experimental measurements of enclosure strain via digital image correlation (DIC).

1.2 BACKGROUND

The concept of employing an evacuated or low pressure enclosure to enhance the thermal performance of flat-plate solar collectors is a concept which dates back to the 1970s (Eaton and Blum, 1975). At this time flat-plate solar collectors were limited in their achievable performance; with efficiencies usually less than 40% for absorber plate temperatures greater than 100°C. Eaton and Blum (1975) suggest that the use of only a moderate vacuum environment (~150 – 3,500 Pa) between the absorber plate and

enclosure glass cover is sufficient to allow the collector to efficiently operate at temperatures exceeding 150°C. Achieving higher temperatures would allow flat plate collectors to be considered for process heat applications. The moderate vacuum pressure range, while being sufficient to effectively suppress convective heat transfer between the absorber plate and the collector glass cover, still allows for gas conduction heat transfer to take place. Gas conduction can account for several Watts of total power loss from a solar collector per unit area depending on the temperature difference between the absorber plate and glass cover (Benz and Beikircher, 1999). Subsequently, it is desirable to attain a vacuum pressure between the absorber plate and glass cover of less than 0.1 Pa in order to fully suppress both convection and gas conduction processes and maximize solar collector thermal performance.

Attaining and maintaining enclosure pressures below 0.1 Pa for an adequate product lifetime (greater than 20 years), represents a significant engineering challenge for a FP collector geometry. This is especially the case when the vacuum layer volume is very small; as in the case of vacuum glazing, which typically employs vacuum layers less than 0.5mm thick (Eames, 2008). To this end, the design of the evacuated enclosures should protect the glass cover and sealing material from the large stresses imposed by atmosphere pressure forces and stresses due to differential thermal expansion between the various enclosure components that could lead to fracture.

Stress in vacuum glazing like structures has been investigated extensively in the literature. Fischer-Cripps et al (1995), utilise analytic and finite element methods, validated via experimental measurements, to characterise the magnitude of stresses induced in vacuum glazing due to the separate influences of atmospheric pressure loading and temperature differentials from one side of the glazing to the other. Simko et al (1998) investigate how mechanical edge constraints on vacuum glazing impact the spatial distribution of stresses in the glazing when subjected to extreme temperature differentials. An experimental and theoretical study by Wang et al (2007) explores the stresses induced in a vacuum glazing that has been fabricated at low temperatures using indium as an edge sealing material.

1.3 CONFIGURATION AND PERFORMANCE

Conventional flat-plate solar collectors are typically configured as depicted in Figure 1. As can be observed in Figure 1, the absorber plate and heat removal tubes are insulated on the rear side of the absorber and on the front side there is an air gap between the absorber and glass cover. For such collectors convective heat loss between the absorber and glass cover can be significant. Typically, heat loss from the collector is characterized by the collector overall loss coefficient (U_L), where U_L is calculated as:

$$U_L = U_t + U_b + U_e \qquad (1)$$

where U_t is the top loss coefficient, U_b is the back loss coefficient and U_e is the edge loss coefficient (see Figure 3). The VFP configuration under consideration in this paper is depicted in Figure 3:

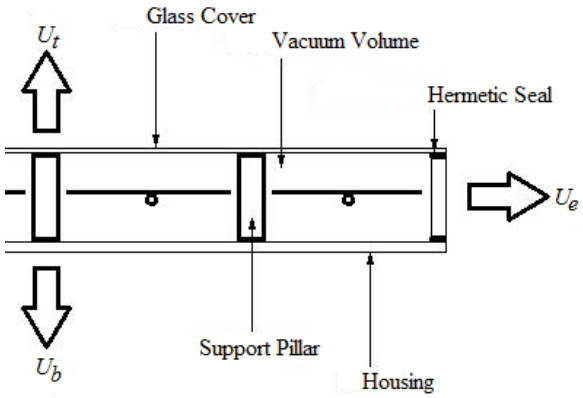

Figure 3: VFP configuration

In this VFP configuration the absorber plate is suspended within the housing such that it is completely surrounded by vacuum, suppressing convection and gas conduction heat loss. An array of support pillars is required to allow the glass cover and housing to resist atmospheric pressure loading resulting from the evacuated volume within the collector. Subsequently, a large overall decrease in heat loss is expected, resulting in the VFP collector operating more efficiently at higher temperatures. This increase in efficiency with decreasing enclosure pressure is described by (Moss and Shire, 2014) and suggests significant improvement of efficiency for VFP collectors, in comparison to FP collectors, of ~ 30-40% at average absorber plate temperatures of 150 K above ambient. It is anticipated that this efficiency would be competitive with evacuated tube solar thermal collectors, however, a VFP collector would employ an absorber which fills a much larger proportion of the available gross collector aperture area. This improved performance suggests that a VFP collector will be suitable for a wide range of applications such as domestic hot water/space heating and process heat production at a range of temperatures. The vacuum insulation layer within the enclosure and surrounding the solar absorber can be very thin whilst still remaining effective; as no bulky backing insulation is required this allows the collector itself to be only slightly deeper than the depth of the solar absorber plate. A thin, light weight collector could be easily mounted onto existing roof structures or as a fascia/façade element on residential or industrial buildings.

1.4 HERMETIC SEALING MATERIALS

A contiguous and robust hermetic seal is required between the glass cover and the collector housing to maintain the vacuum within a VFP collector over its lifetime. This type of sealing is akin to that in vacuum glazing, for which there are several candidate materials (Eames, 2008). A primary factor in the selection of candidate materials is the seal material softening temperature. If the softening temperature is in the range 300-400°C or higher, then there is a significant likelihood that a tempered glass cover would lose temper during the sealing process and any low-emissivity coatings applied to the glass cover may degrade (Eames, 2008). If the softening temperature of the seal material is relatively low in comparison to the stagnation temperature of the solar collector then

there is a significantly higher risk that the seal will fail over the product lifetime. Conventional materials which have been considered for vacuum glazing include solder glass and indium solder alloys (Eames, 2008).

Indium solder has a softening temperature of ~154°C and is bonded to glass and metal surfaces via ultra-sonic soldering. The sealing technique involves placing two indium coated surfaces together and baking. At this temperature the indium is able to sub-duct the surface oxide layer at the joint interface resulting in mixing of the indium bonded to the two components forming a seal between them. This technique, as described in (Eames, 2008), works well for vacuum glazing. However, indium would pose a greater risk of seal failure, due to its low melting point, for a VFP collector. This is especially true around the inlet and outlet ports of the collector. Nonetheless, assuming that the collector operation stagnation temperature is not too high and the seal is thermally insulated from the flat plate absorber, indium is a feasible seal material.

A range of tin based solders are also considered for this application. One such solder is S-bond 220M, which is a solder alloy consisting of tin, titanium, silver and magnesium (S-Bond, n.d.). This particular alloy has a softening temperature from 240 - 260°C. Another example of a tin based solder is Cerasolzer 220 which was a softening temperature at around 220°C (MBR-Electronics, 2009). The sealing technique is similar to that of indium, however, tin based solders also require surface dross skimming and mechanical activation to break down the surface oxide layer to form the seal; thus further complicating the sealing process.

1.5 MODELLING APPROACH

The modelling approach used in this study is similar to that employed by Wang et al (2007) and Simko et al (1998) to investigate pressure and temperature induced stresses in vacuum glazing. The approach used in these cases are validated against the experimental results of Simko et al (1998) and Fischer-Cripps et al (1995).

Stresses on the enclosure are modelled via a parametric analysis in which finite element method (FEM) software (Abaqus) is employed to model the stresses in two enclosure configurations. Elements in the model are 8-node linear 3D stress elements. An initial validation of the modelling approach was conducted via reproduction of several of the results published by Wang et al (2007) and Simko et al (1998). Mesh resolution was refined via comparison of generated data to the reported experimental and simulated results, providing average errors of ~5%; this ensured reliable and realistic stress behaviour could be observed. Comparing the results of Wang et al with results generated via the modelling approach planned for use in the current study, good agreement was observed between the two. Subsequently, it was anticipated that the modelling approach employed for use in the current study would provide stress profiles representative of what would be seen in evacuated enclosure for flat plate solar collectors.

2 STRESSES IN EVACUATED ENCLOSURES

The enclosure concept considered in the current project is similar to vacuum glazing, however, a flexible metal tray (of depth between 10-20mm) is bonded to the front glass cover to create a deeper volume vacuum enclosure. This subsequently requires larger

pillars to support the top glass cover (see Figure 2). Although different to vacuum glazing, it is expected that, given the similar nature of the structure to vacuum glazing, a similar analysis can be conducted to assess stress resulting from atmospheric pressure loading and differential thermal expansion as was conducted previously for vacuum glazing (Simko et al., 1998).

2.1 Stress due to Atmospheric Pressure:

When considering stresses induced in an enclosure due to atmospheric pressure compressing the structure, the main region of concern is the stress induced in the glass cover resulting from the indentation of a support pillar, in particular the tensile stress induced on the exterior surface of the glass cover (Collins and Fischer-Cripps, 1991). Qualitatively, it can be reasoned that this type of stress occurs closely in the vicinity of a support pillar; as is the case for vacuum glazing (Collins and Fischer-Cripps, 1991). These stresses, as they occur in the centre of the glass cover, can be analysed using a FEM geometry as seen in Figure 4 a and b, where symmetry boundary conditions are applied around the periphery of the geometry, an atmospheric pressure load is applied to the top and bottom surfaces. Figure 5 shows the stress profile on the exterior surface of the glass as generated by the FEM model for two pillar spacing sizes.

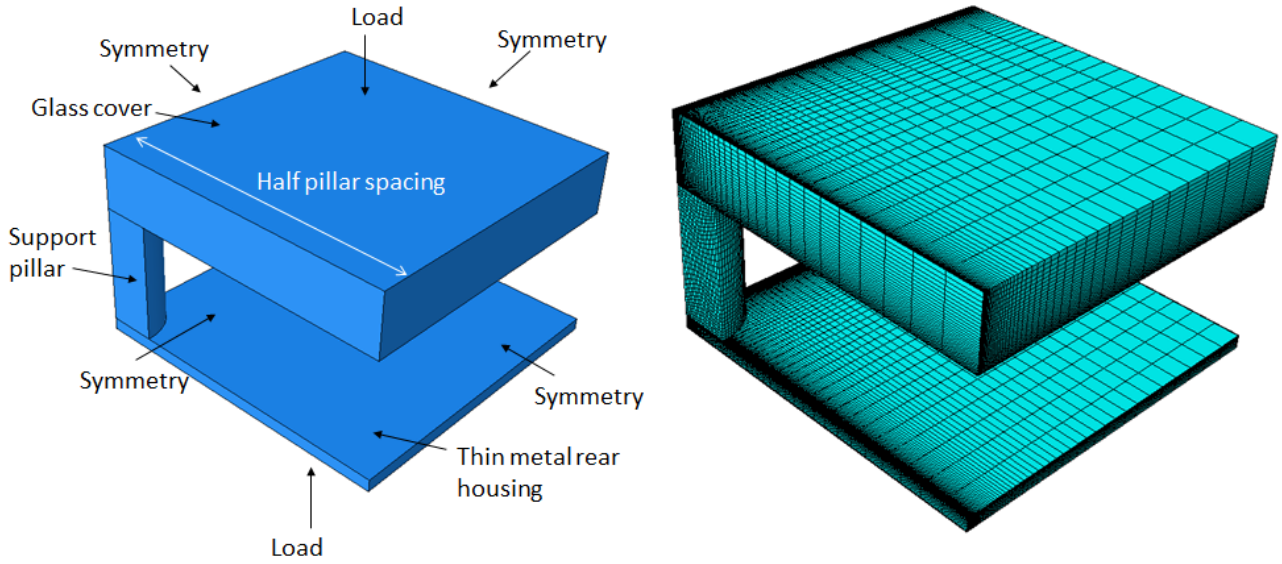

Figure 4: Central glass cover stress (a) FEM model geometry (b) computational mesh

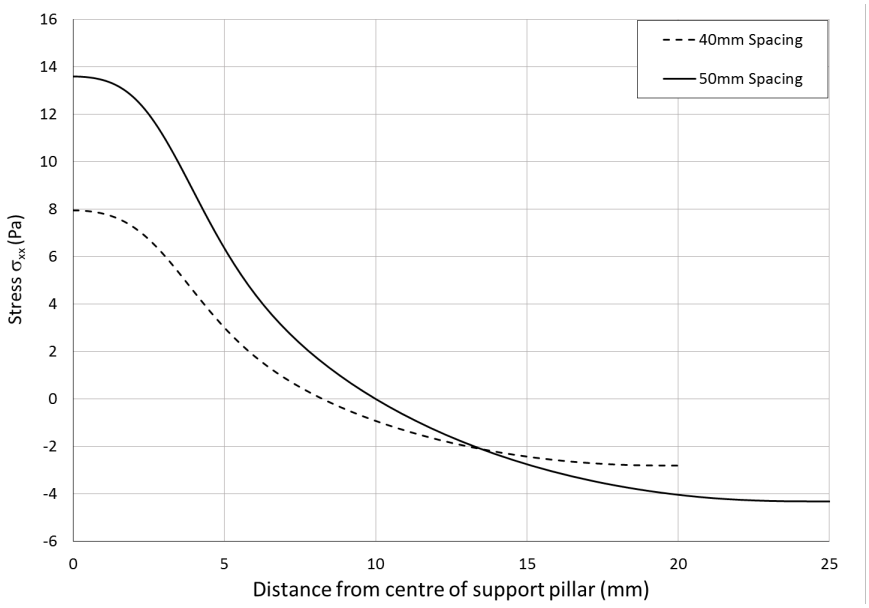

Figure 5: Atmospheric pressure induced stress on external glass cover surface in vicinity of support pillar for 40 and 50mm pillar spacing

2.1.1 Pillar Array Constraints:

As the evacuated enclosure concept s is similar to vacuum glazing configurations, many of the design constraints for vacuum glazing are transferable. These constraints include limits on: external glass cover surface tensile stress, internal glass cover stresses for the prevention of Hertzian cone fractures and compression forces on the support pillars; all of which are induced via atmospheric pressure loading. These constraints are met by careful selection of support pillar array parameters, which include support pillar, radius (a) and spacing (λ). A further parameter which might be varied is the glass covers thickness. The glass cover thickness will serve to reduce the level of stress the exterior surface of the glass is exposed to as it is increased. Initially, in this study, the glass cover thickness was kept constant at 4mm, this being the same thickness utilised in most vacuum glazing (Eames, 2008; Wang et al., 2007). Furthermore, the support pillar height was kept constant at 10mm as it was thought that the height of the pillar would not impact the stress experienced by the glass cover due to atmospheric pressure loading.

A conservative limit on the glass cover external stress is discussed by (Collins and Fischer-Cripps, 1991) and should not exceed 8 MPa for standard annealed glass and if possible kept below 4 MPa over the majority of the external glass cover surface as this would significantly reduce the risk of glass fracture formations. Tempered glass is expected to be approximately 4-5 times stronger than standard annealed glass suggesting that the majority of external glass cover surface should be kept below a stress level of 20 MPa. In this study it is assumed that tempered glass is a valid choice for both enclosure concepts and therefore the 20 MPa stress limit was selected as a design criteria. External tensile stress on the glass is determined via a parametric analysis in which geometries representative of different combinations of pillar radius and spacing are modelled via finite element analysis, examples of which are seen in Figure 4.

Internal glass cover stresses can be found when considering Auerbach's law; based upon which Fischer-Cripps and Collins (1991) propose the following relation:

$$\lambda = \frac{1}{q^{1/2}}\left[\frac{E\pi^3\beta\gamma a^3}{(1-\mu^2)2\Phi_a}\right] \qquad (2)$$

where E is the Young's Modulus of the glass cover, β is an empirical friction factor, γ is the fracture surface energy (3.6 Jm^{-2} for soda lime glass) and Φ_a is the value of the strain energy release function where it plateaus in the Auerbach range (0.0013 for soda-lime glass).

It is important to also consider the compressive stress in the support pillars themselves. The vacuum enclosure support pillar array size and spacing should be selected such that the compressive stress (σ) on the pillars does not exceed the compressive strength of the pillar material. The relationship between pillar separation and pillar radius for a given compressive stress is given by:

$$q\lambda^2 = \sigma\pi a^2 \qquad (3)$$

where q is the atmospheric pressure load. A final constraint identified specifically for VFP collectors is a limit on total pillar array area such that a large proportion of area is available within the vacuum enclosure for the collector absorber plate to occupy. In the current study, this limit on pillar array area is set to 3% of the available area in the collector.

When considering all these mechanical design criteria, a range of safe values for a and λ can be identified graphically similar to the procedure described by (Collins and Fischer-Cripps, 1991).

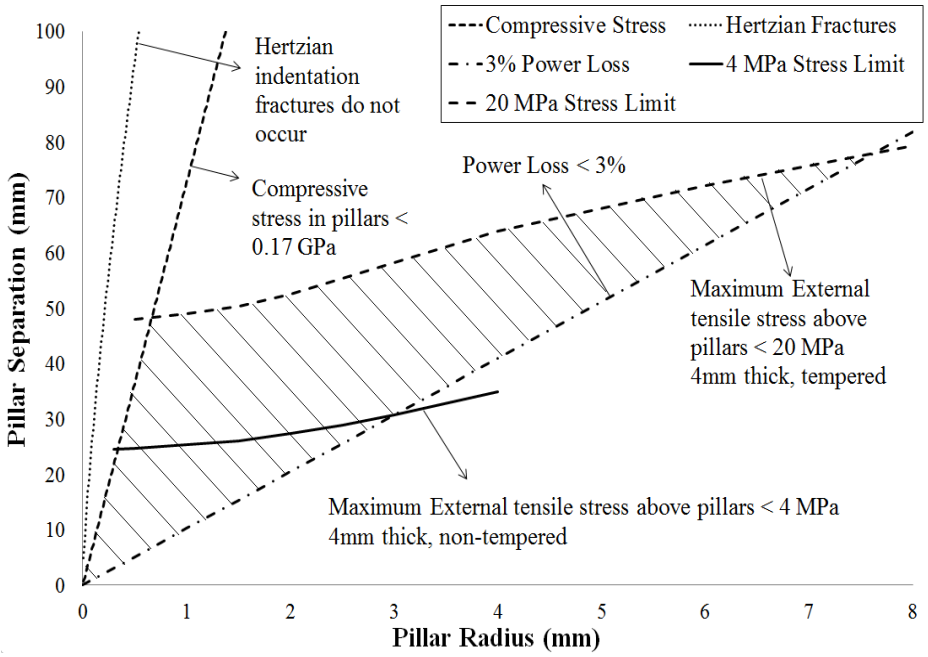

Figure 6: Pillar array design safety envelope for tempered and non-tempered glass

In Figure 6, acceptable combinations of the design parameters (a and λ) can be found within the shaded region bound by the various

constraint curves. From Figure 6, maximum values of a and λ are found for both annealed and tempered glass. It should be noted that these analyses are representative of stresses in the centre of the panel due only to atmospheric pressure loading for 4mm thick glass. Stresses imposed via differential thermal expansion of the enclosure components will result in a shift in the intensity of stress experienced by the glass cover. The impact of this is discussed in the next section.

2.2 Modelling and experimental considerations:

Stresses are also induced in the enclosure due to differential thermal expansion of the different enclosure components. These stresses will occur when the enclosure is cooled below the solidus temperature of the sealing material used and also when the enclosure is non-uniformly heated with the glass cover being at a different average temperature to the rear metal housing. For the enclosure concept under consideration thermal expansion stresses can be visualised as seen in Figure 7:

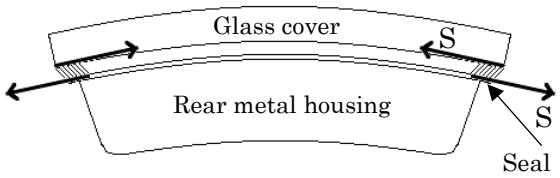

Figure 7: Forces due to differential thermal expansion of the enclosure components.

In Figure 7 it can be seen that there will be a finite bending moment resulting in the structure being bent in to a spherical shape. This is due to the different thermal expansion coefficients of the glass cover and metal tray components in a similar fashion to the bending experienced by vacuum glazing, as described in (Wang et al., 2007). Depending of the thermal radiative properties of the various enclosure components it is possible that the rear metal housing will be slightly cooler or warmer than the glass cover during collector operation, subsequently it is particularly important to select materials for this concept of enclosure that have similar coefficients of thermal expansion.

The shear force/unit length (S) along the edge of the enclosure and the radius of curvature (R) of the enclosure can be estimated analytically via consideration of laminated slabs. This is similar to the analytical analysis conducted by Collins et al (1992), however, in this case the different slabs (denoted by subscripts *1* and *2*) are at the same temperature (T), cooler than the stress free temperature (T_{ref}), and have different expansion coefficients (α). This results in equation 18 of (Collins et al., 1992) becoming:

$$S = \frac{\alpha_1\left(T - T_{ref}\right) - \alpha_2\left(T - T_{ref}\right)}{\frac{\left(1-\mu_1\right)}{t_1 E_1} + \frac{\left(1-\mu_2\right)}{t_2 E_2} + \frac{3\left(t_1 + t_2\right)^2}{\left[\frac{E_1 t_1^3}{\left(1-\mu_1\right)} + \frac{E_2 t_2^3}{\left(1-\mu_2\right)}\right]}} \qquad (4)$$

Here t is the slab thickness, E is the slab young's modulus and μ is the slab Poisson ration. The associated radius of curvature is then estimated as:

$$R = \frac{1}{6S(t_1 + t_2)}\left[\frac{E_1 t_1^3}{(1-\mu_1)} + \frac{E_2 t_2^3}{(1-\mu_2)}\right] \quad (5)$$

In modelling stresses due to differential thermal expansion of the components of an evacuated enclosure it is important to know the expected temperature of the enclosure. A simple worst case scenario was used to assess enclosure stresses in which tin based solder is used with a solidus temperature of 220°C. The enclosure is cooled to a temperature of -20°C, representative of extreme winter conditions, resulting in a 240°C temperature difference from the stress free temperature of 220°C. The stresses due to differential thermal expansion and atmospheric pressure loading of the enclosure are modelled via FEM analysis. In this set of analyses the metal tray component of the enclosure has a thermal expansion coefficients consistent with 400 series stainless steel. This metal was selected due its relatively low thermal expansion coefficient of 10.8×10^{-6} K^{-1}, which is close to that of soda-lime glass (8.9×10^{-6} K^{-1}). The dimensions of the enclosure components were based on a prototype square enclosure measuring 0.5m in length, fabricated at Loughborough University (Figure 8a). In this case the glass cover thickness is 4mm, the tray depth is 10mm, the seal area is 8.9mm and the metal tray has a thickness of 0.8mm. The support pillars are 6mm in diameter and spaced at 60mm intervals. The quarter geometry used for these FEM models is shown in Figure 8b. This combination of pillar size and spacing was selected as it represents a combination that is in the vicinity of the 20 MPa limit of Figure 6 and allows for better measurement of stresses in the fabricated enclosure via digital image correlation due to the large amount of strain expected. In the following sections the results of this FEM analysis are presented combined with experimental measurements of the strain experienced by the enclosure due to atmospheric pressure loading.

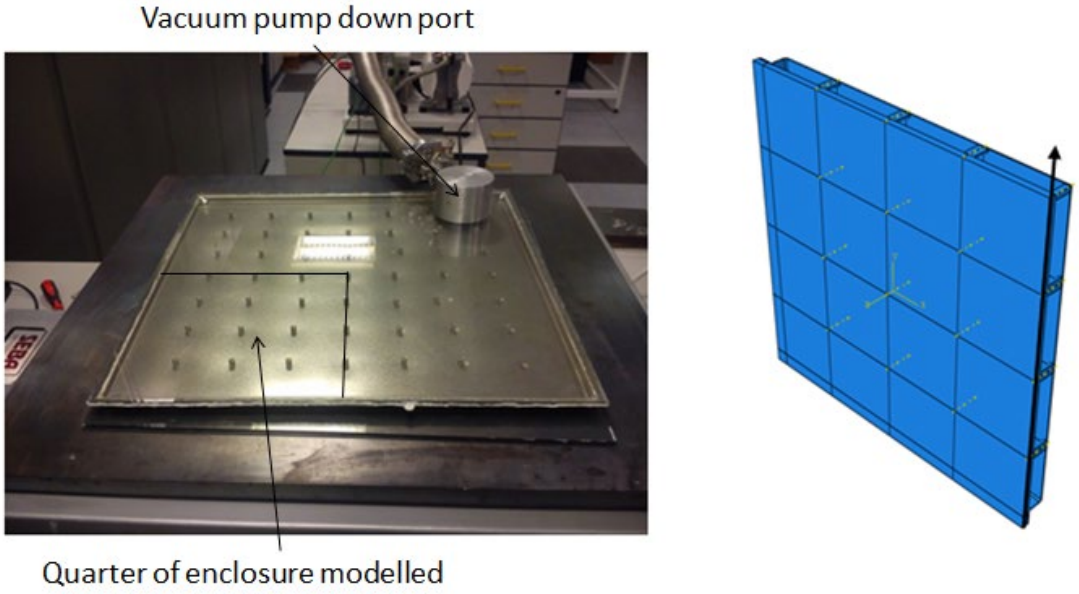

(a) (b)

Figure 8: (a): Fabricated 0.5x0.5m metal tray enclosure; (b): FEM metal tray enclosure geometry

2.3 Digital Image Correlation Strain Measurements of the Evacuated Enclosure:

Digital image correlation (DIC) equipment, Dantec Dynamics Q-400 DIC, was used to measure the strain profile over the surface of the 0.5x0.5m fabricated enclosure depicted in Figure 8. The DIC operates via comparing images of the enclosure taken via two separate high resolution digital cameras. The measurement requires the glass cover of the enclosure to be spray painted to produce a random black specked pattern on a white background. The DIC system was calibrated via a standard method as outlined by Dantec and utilised standard industry image correlation parameters for the evaluation of surface strains (DANTEC-Dynamics, 2014). The DIC equipment setup is depicted in Figure 9 where it is necessary to coat the surface of the enclosures glass cover with a random black speckle pattern on a white background. A preliminary experiment was conducted with the DIC in which images were taken of the fabricated and sealed enclosure prior to evacuation and then again after evacuation to ~5,000 Pa, which results in a pressure of 96,325 Pa being applied to the outside surfaces of the enclosure (96% that of atmospheric pressure). This experiment was conducted at room temperature and subsequently the strain profile resolved by the DIC, of the glass cover, is attributable only to atmospheric pressure loading. Further experiments will be conducted to investigate enclosure strains due to differential thermal expansion of the enclosure and this will be the subject of later papers.

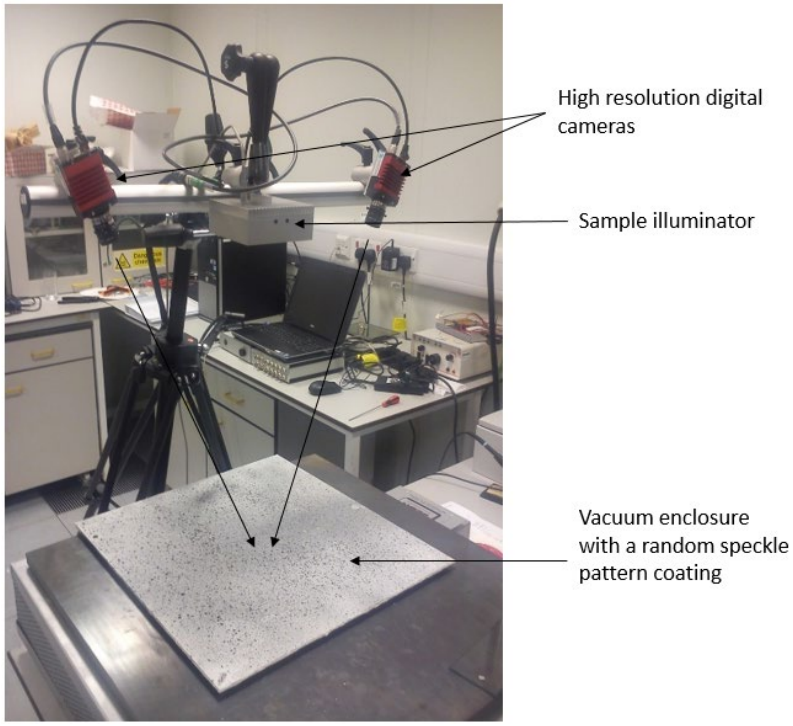

Figure 9: DIC equipment setup for measurement of evacuated enclosure strain.

From the preliminary experimental measurements described, principal strain contours were resolved of the glass cover surface in which the impact of the support pillars is clearly visible, as shown in Figure 10 :

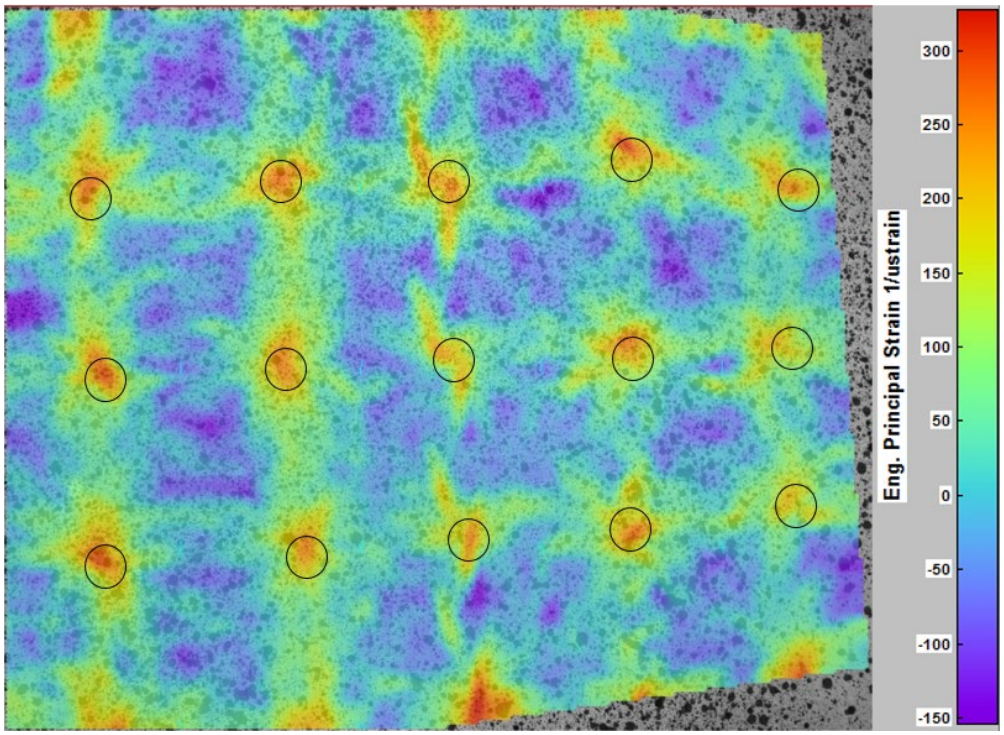

Figure 10: DIC principal strain contours, circles indicate locations of pillars.

Similar and consistent principal strain contours were produced via a FEM simulation of the enclosure in which only atmospheric pressure forces were acting on the enclosure structure; these are seen in Figure 11.

From the data produced via the DIC, focus was given to comparing the measured tangential strain components, ε_{11} and ε_{22}, in the vicinity of the support pillars with those produced via the FEM simulation. Measured tangential strain components were found to be consistent with those predicted; an example of this is seen in Figure 12 in which ε_{11} strain profiles in the vicinity of a support pillar, moving in the y direction, are compared.

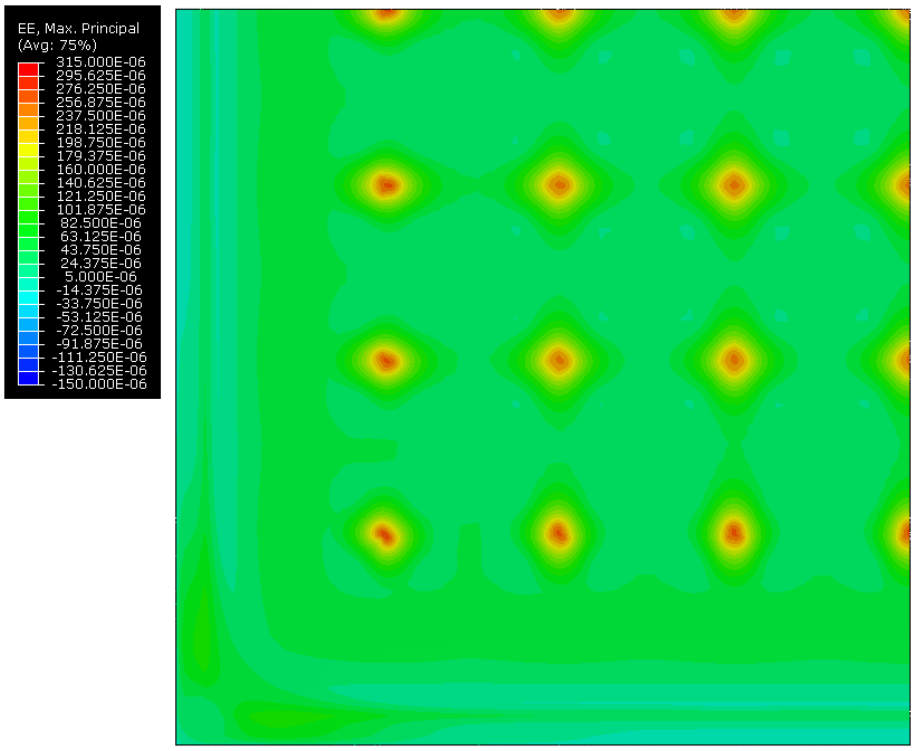

Figure 11: Principal strain contours produced via FEM simulation

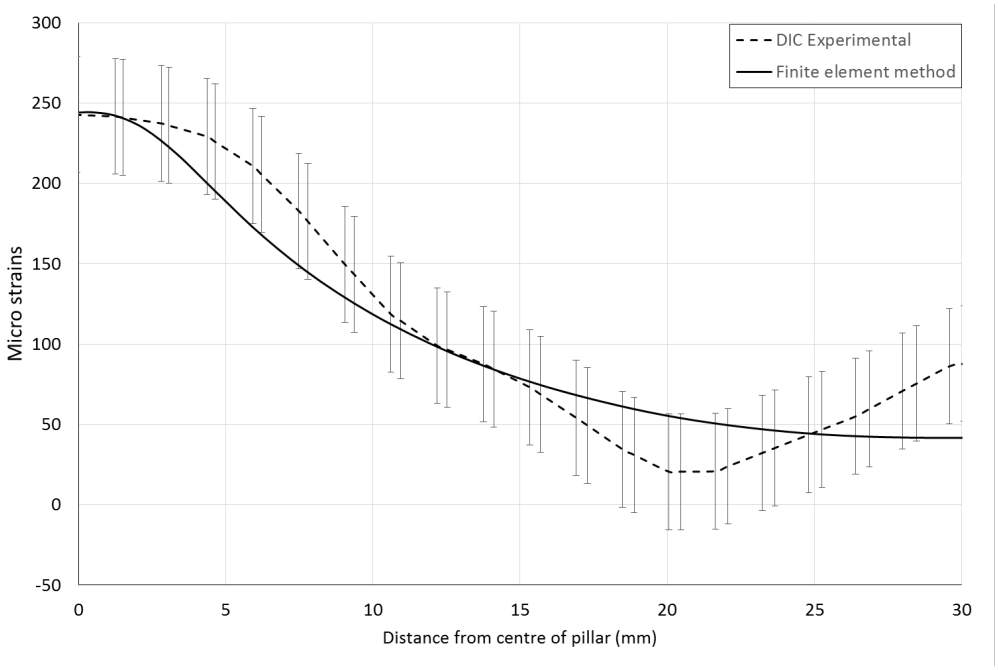

Figure 12: ε_{11} strains in the vicinity of a support pillar taken along the y (vertical) direction.

From the results of the preliminary experiment described, as seen in Figure 10 and Figure 12, good agreement, within the error bounds, was observed between simulation and experiment validating the current FEM modelling approach and providing confidence in further FEM simulation predictions.

2.4 FEM modelling of enclosure stress due to differential thermal expansion and atmospheric pressure loading:

For the FEM analysis of the enclosure, focus was given to reporting tangential stress components (σ_{11} and σ_{22}) and surface normal deflections, resulting from the combination of stresses induced via differential thermal expansion and atmospheric pressure loading, of the external surfaces; as these parameters are most likely to drive failure mechanisms (Collins and Fischer-Cripps, 1991). The FEM analyses considered the case of the enclosure being 240°C cooler than the stress free temperature of 220°C. Predicted stress components for this simulation were compared to predicted stress components, for the same geometry, in the case of the enclosure only being stressed via atmospheric pressure loading. The surface normal deflections of the glass cover of the enclosure is also compared to that predicted by the analytical bending model of equations 4&5. Predicted tangential stress component data was extracted along a line on the external surface of the glass cover 250 mm from the edge spanning from one edge to the centre of the enclosures, this is depicted via the arrows in Figure 8. The deflections of the enclosure for these cases are plotted and in Figure 13 and the corresponding tangential stress components are plotted in Figure 14:

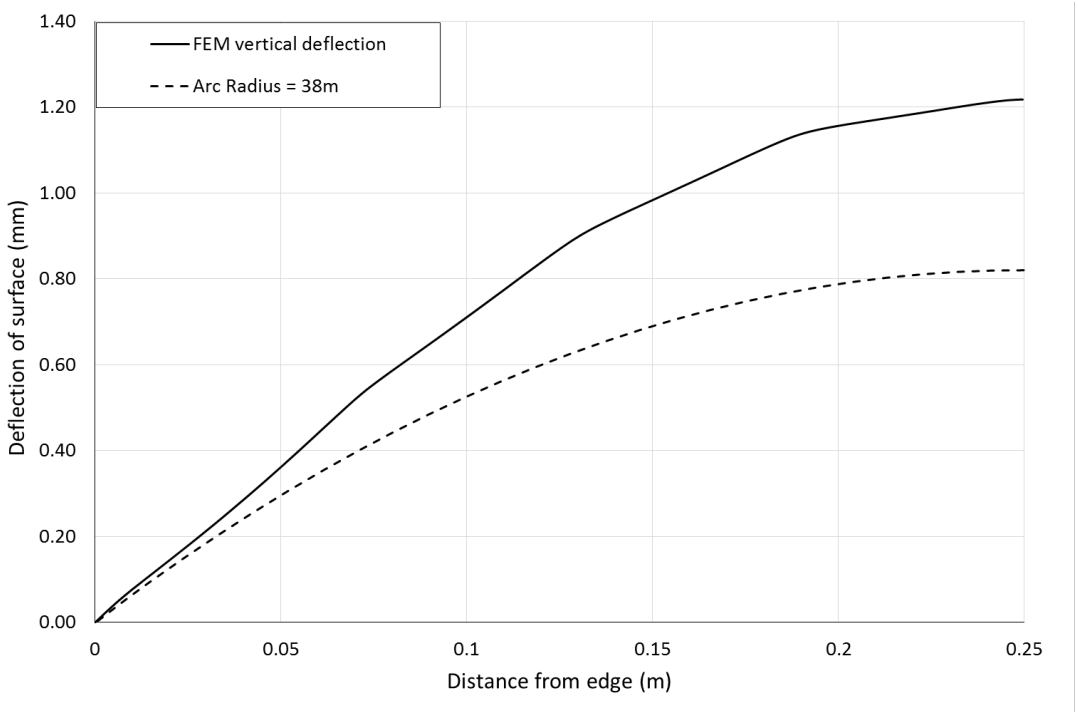

Figure 13: Predicted vertical deflections of external glass surface

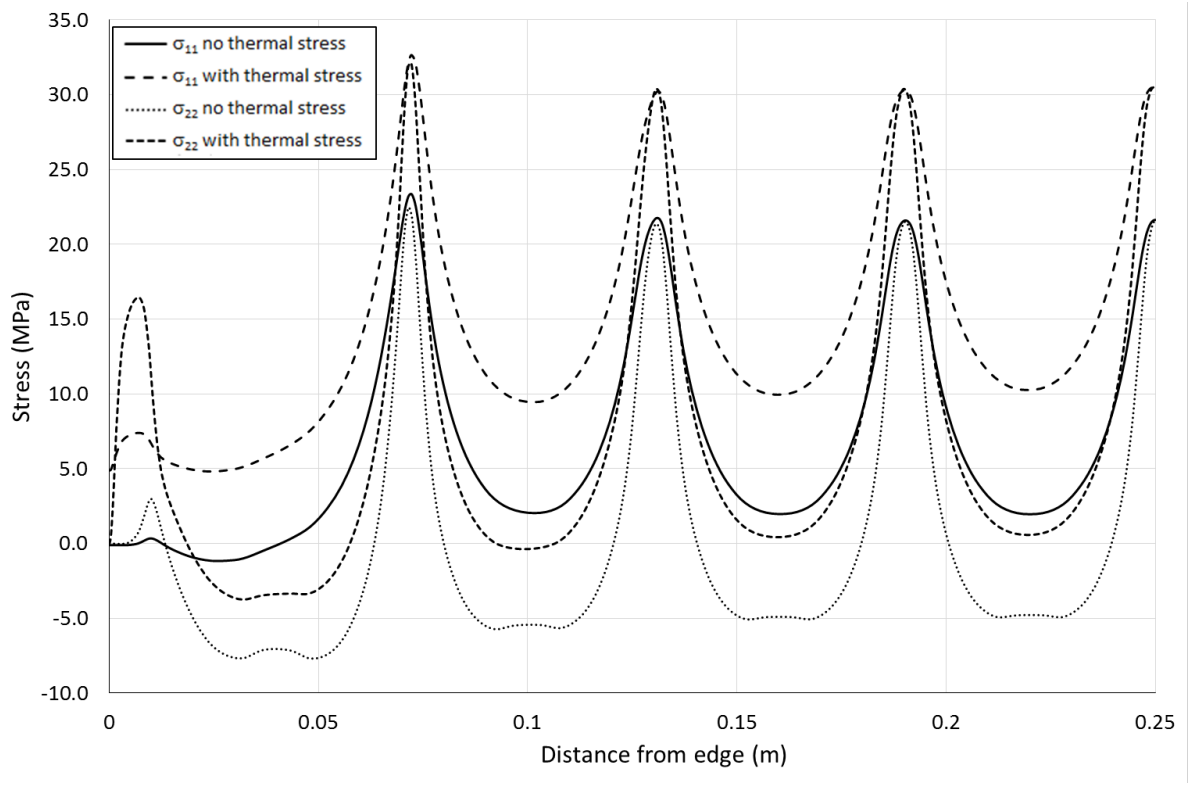

Figure 14: Tangential stress component of external glass surface

The tangential stress components plotted in Figure 14 illustrate the impact of the additional stress due to the differential thermal expansion of the enclosure components. Peak tangential stresses are slightly in excess of the 20 MPa limit in the case of no thermal stress. Peak tangential stresses are observed to increase by 8-12 MPa with the inclusion of differential thermal expansion behaviour in extreme winter conditions. The largest increase in peak stresses is observed close to the enclosure edge.

A significant level of deflection of the enclosure is observed as seen in Figure 13, with a maximum estimated vertical deflection of 1.2mm. Equations 4 and 5 underestimate this deflection by ~30%, this is likely due to the assumption of a slab structure, inherent in the equations, which would result in a stiffer composite structure. Consideration should be given to the deflection experienced by the enclosure when considering the integration of this type of enclosure with buildings. Any frame or support structure for this type of enclosure will have to allow for the change in shape of the enclosure with varying environmental temperature and operating conditions. It is likely that with larger sized enclosures, compared to enclosure geometries depicted in Figure 8, the magnitude of deflection experienced by the enclosure will be greater.

With the inclusion of differential thermal expansion stresses it is clear that this configuration of parameters for the enclosure is likely to be unsuitable for an evacuated flat plate solar collector. The geometry of enclosure modelled, seen in Figure 8, is representative of enclosures being fabricated for experimental testing. It is of interest, however, to model the deformation and stress in enclosures whose dimensions are similar to that of conventional solar thermal collectors. This allows for the examination of how much deflection is likely to occur when conventionally sized vacuum solar thermal collectors are subject to significant thermal stress

as well determining how peak stresses in the glass cover might change for a larger sized enclosure. Subsequently, a larger FEM quarter geometry was constructed for both enclosure concepts representative of a 1 m^2 vacuum solar collector. Given that the previous smaller sized geometry exhibited peak stresses in excess of the 20 MPa limit, some parameters were altered to reduce the stress experienced by the glass cover. Specifically, this involved a reduction in pillar spacing and an increase in glass thickness. The enclosure used 6mm diameter support pillars, with 100 support pillars being included in the quarter geometry at a pillar spacing of 50mm. Considering the deflections and stress seen in the external glass cover for the small enclosure geometries it was decided that a 6mm glass cover would be used to reduced external surface stresses as well as a 1mm thickness for the metal tray. This model geometry is depicted in Figure 15.

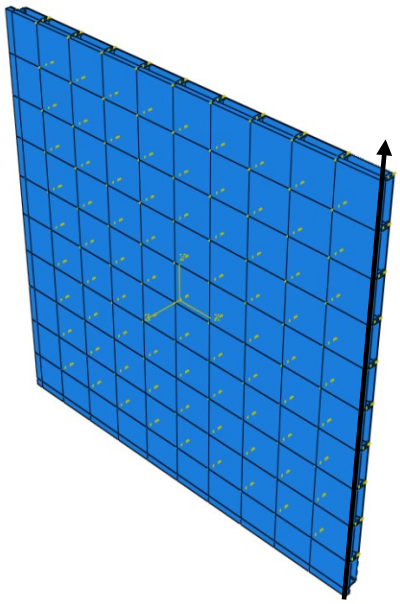

Figure 15: FEM quarter geometries for 1x1m enclosure

In conducting these FEM analysed for the larger size geometry it was found that the enclosure is again subject to spherical bending as observed in Figure 16. The magnitude of the deflection in this case is approximately 4.8 mm; a circular arc with radius (32 m) calculated by equation 5, is also plotted and predicts a deflection relatively consistent with the magnitude of the FEM result. Figure 17 plots the tangential stress components of the external glass cover along a centre line of the geometry starting at the edge and moving to the centre as depicted by the arrows of Figure 15. In Figure 17 the impact of the thicker 6mm glass is clear with the enclosure exhibiting tensile stress peaks less than the 20 MPa limit. Interestingly, the impact of the differential thermal expansion is again seen to increase peak stresses by ~ 8-12 MPa. Finally, it is observed in Figure 17 that tensile stress peaks level out at around 0.2m, as the centre of the enclosure is approached. These results suggest that this configuration of enclosure parameters would likely be suitable for a conventionally sized evacuated flat plate solar collector.

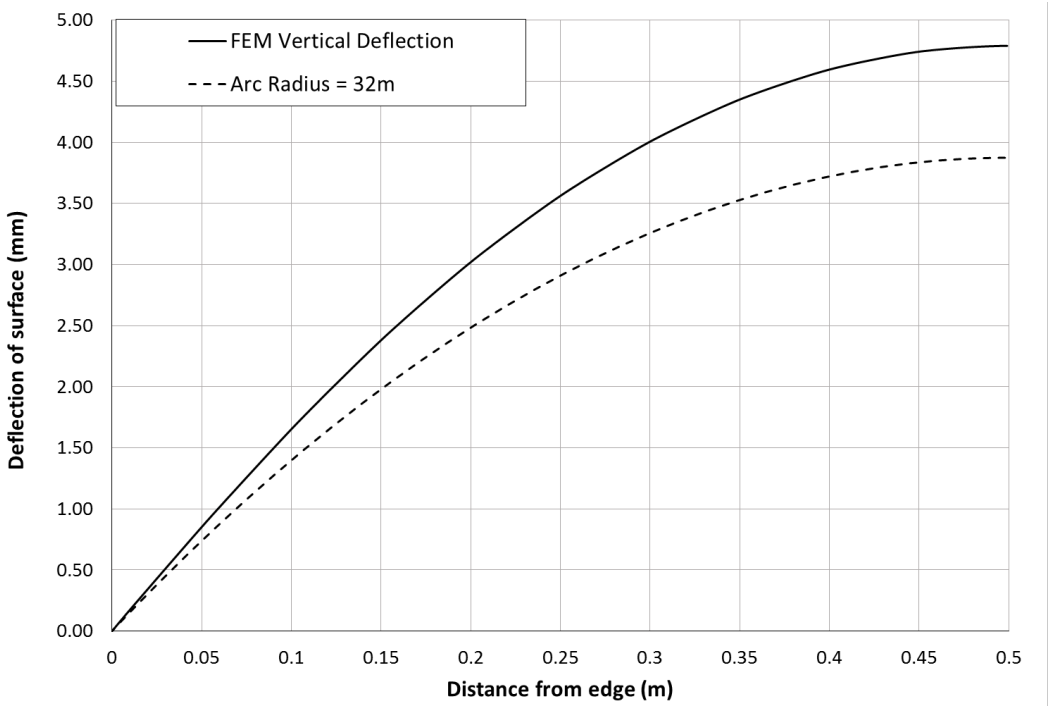

Figure 16: Vertical deflections of external glass surface for 1x1m enclosure

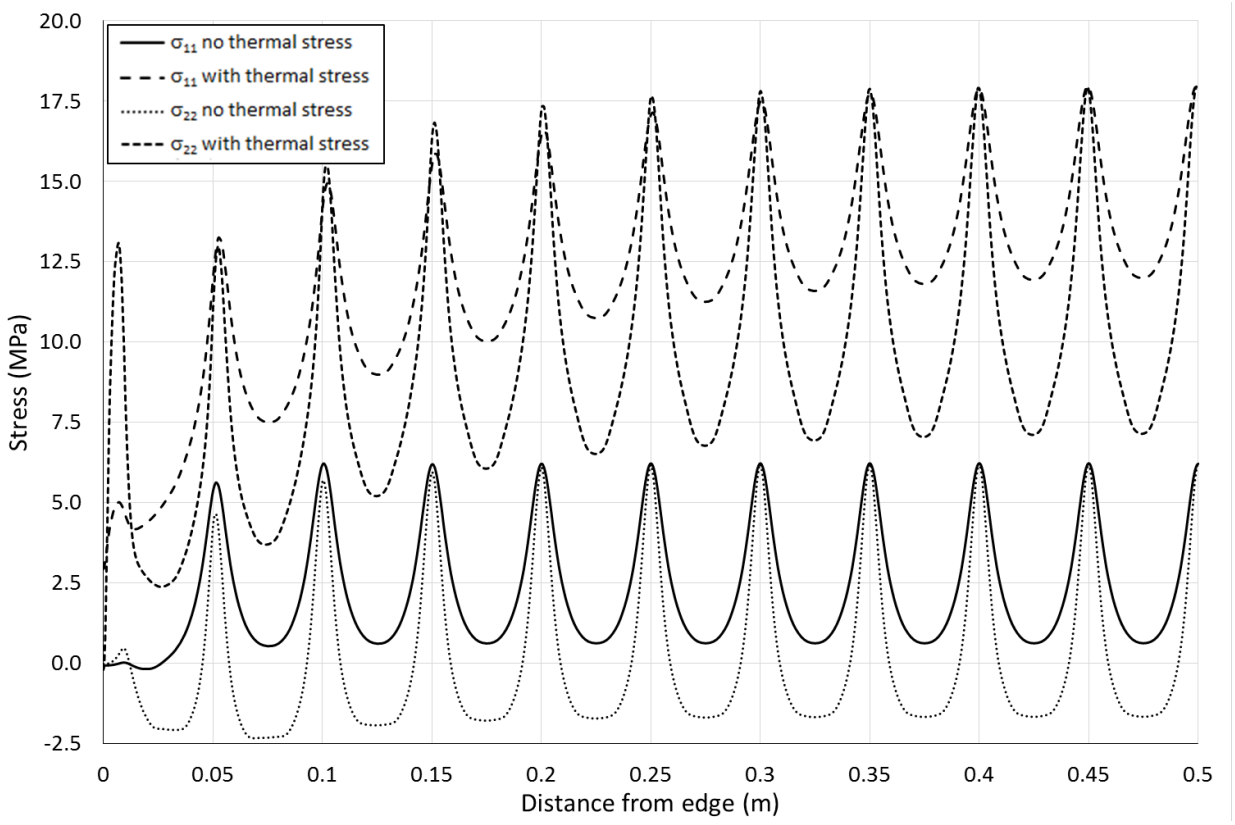

Figure 17: Tangential stress component of external glass surface for 1x1m enclosure

CONCLUSIONS

Durable vacuum enclosure structures for flat plate evacuated solar thermal collectors are a critical component in ensuring the collector is safe and robust to environmental conditions, while also helping to ensure the required vacuum environment is maintained for the lifetime of the collector. The enclosure concept identified in this paper is found to be susceptible to stresses imposed by differential thermal expansion, however, it is expected that the produced concept could more easily utilise tempered glass within its structure. With correct selection of enclosure mechanical design parameter this enclosure concept should be able to withstand sustained stress due to atmospheric pressure loading and differential thermal expansion resulting from exposure to winter conditions with no damage.

From finite element analyses conducted it was apparent that the enclosure will be subject to significant and continuous differential thermal expansion stresses, particularly when subjected to winter conditions. Use of metals such as 400 series stainless for the rear collector housing and 6mm tempered glass for the collector front cover, resulted in acceptable levels of additional thermal stress in the structure. Finite element analyses of a 1x1m enclosure with a 6mm glass cover predicts that tensile stress peaks on the external glass cover in the vicinity of support pillars level off to a particular stress level over a distance of around 0.2m. Preliminary experimental = measurements of glass cover surface strain were found to be consistent with FEM simulation results. Further work is necessary to experimentally characterise stresses in evacuated enclosure concepts and further validate finite element models. It is likely that these enclosures will be subject to more complex environmental and operational conditions than considered in this analysis. Such conditions include induced stresses during collector operation for a variety of environmental conditions and investigating the impact of short duration external loads which may result from windy conditions or physical impact from external factors. However, based on the results of this study it is anticipated that, with suitable selections of design parameters, this enclosure concept will be robust to a variety of scenarios whilst effectively supporting the operation of evacuated flat plate solar thermal collectors as a versatile renewable energy building component.

ACKNOWLEDEGMENTS

This project was supported by the Engineering and Physical Science Research Council within the High Performance Vacuum Flat Plate Solar Thermal Collector for Hot Water and Process Heat project (EP/K009230/1)

REFERENCES

Benz, N., Beikircher, T., 1999. High efficiency evacuated flat-plate solar collector for process steam production. Sol. Energy 65, 111–118.

Collins, R.E., Fischer-Cripps, a. C., Tang, J.-Z., 1992. Transparent evacuated insulation. Sol. Energy 49, 333–350. doi:10.1016/0038-092X(92)90106-K

Collins, R.E., Fischer-Cripps, A.C., 1991. Design of Support Pillar Arrays in Flat Evacuated Windows. Aust. J. Phys. 44, 545–564.

DANTEC-Dynamics, 2014. Q-400 Systems Operation Manual.

Eames, P.C., 2008. Vacuum glazing: Current performance and future prospects. Vacuum 82, 717–722. doi:10.1016/j.vacuum.2007.10.017

Eaton, C.B., Blum, H. a., 1975. The use of moderate vacuum environments as a means of increasing the collection efficiencies and operating temperatures of flat-plate solar collectors. Sol. Energy 17, 151–158. doi:10.1016/0038-092X(75)90053-5

Fischer-Cripps, a. C., Collins, R.E., Turner, G.M., Bezzel, E., 1995. Stresses and fracture probability in evacuated glazing. Build. Environ. 30, 41–59. doi:10.1016/0360-1323(94)E0032-M

MBR-Electronics, 2009. Active Solder Alloy CERASOLZER [WWW Document]. URL http://www.cerasolzer.com/cerasolzer/cerasolzer_gb.html. (accessed 2.18.15).

Moss, R., Shire, S., 2014. Design and Performance of Evacuated Solar Collector Microchannel Plates, in: EuroSun.

PressGlass, n.d. Thermally Toughened Glass : Flatness and Roller Wave Distortion [WWW Document]. URL http://www.gilje.no/media/113056/Thermally Toughened Glass - Flatness and Roller Wave Distortion.pdf (accessed 2.17.15).

S-Bond, n.d. S-Bond Technologies Products [WWW Document]. URL http://www.s-bond.com/products/. (accessed 7.27.15).

Simko, T.M., Fischer-Cripps, A.C., Collins, R.E., 1998. TEMPERATURE-INDUCED STRESSES IN VACUUM GLAZING : MODELLING AND EXPERIMENTAL VALIDATION. Sol. Energy 63, 1–21.

TVP-Solar, n.d. TVP Solar Home [WWW Document]. URL http://www.tvpsolar.com/index.php. (accessed 7.15.15).

Wang, J., Eames, P.C., Zhao, J.F., Hyde, T., Fang, Y., 2007. Stresses in vacuum glazing fabricated at low temperature. Sol. Energy Mater. Sol. Cells 91, 290–303. doi:10.1016/j.solmat.2006.10.007